First Demonstration of in Situ Electrochemical Control of a Base Metal Catalyst: Spectroscopic and Kinetic Study of the CO + NO Reaction over Na-Promoted Cu

Federico J. Williams, Alejandra Palermo, Mintcho S. Tikhov, and Richard M. Lambert*

Department of Chemistry, University of Cambridge, Cambridge CB2 1EW, U.K.

Received: July 1, 1999; In Final Form: September 20, 1999

Controlled, reversible electrochemical promotion (EP) of a base metal catalyst has been demonstrated for the first time. Electropumping of Na from a β'' alumina solid electrolyte to a Cu film catalyst results in large improvements in both activity and selectivity of the latter. In the catalytic reduction of NO by CO, the reactive behavior, surface composition, and response to EP are a strong function of the composition of the reactant gas. Electron spectroscopic data show that these effects are due to pumping of Na to the catalyst where, under reaction conditions, it is present as $NaNO_3$ on an oxidized Cu surface. Taken together, the spectroscopic and reactor results show that Cu^0 sites are not of significance and that the catalytically active surface is dominated by Cu^+ and Cu^{2+} sites. They also suggest that Cu^+ is of principal importance for the dissociative adsorption of NO and that EP is due to Na-induced enhancement of the adsorption and dissociation of NO at these sites.

Introduction

Copper-based catalysts for NO reduction have been studied for many years because their low cost offers large potential economic benefits in the field of emission control catalysis.[1] Extensive research on the use of such catalysts for NO reduction carried out in the 1960s and early 1970s[2,3] has been reviewed by Shelef.[4] In this connection, the CO + NO reaction has received the most attention because of its simplicity and relative ease of investigation; a recent comprehensive review is available.[5] There is no generally agreed reaction mechanism, and there are divergent opinions about the nature of the catalytically active site or sites. An important issue concerns the oxidation state of the catalytically active surface. It seems likely that, at least in part, disagreements in the literature reflect the sensitivity of the copper/oxygen system to changes in oxidation potential of the gas phase. With oxygen as oxidant, small changes in O_2 partial pressure can result in abrupt phase transitions between Cu metal, Cu_2O, and CuO, accompanied by pronounced changes in catalytic behavior.[6−11] Furthermore, depending on the rates of oxygen transfer to and from the solid, the catalyst composition may not be uniform as one proceeds from the surface to bulk. With NO as oxidant, similar effects are to be expected, although less pronounced than in the case of O_2. In this connection, it is noteworthy that the steady-state reaction kinetics are essentially the same, regardless of whether the starting material is Cu metal or Cu_2O.[5] A variety of reaction mechanisms has been proposed, often containing a large number of postulated elementary steps and adsorbed species. Some authors have proposed that Cu^0, Cu^+, and Cu^{2+} sites are all involved in catalytic turnover.[12] Others have suggested[13] that adsorbed nitrogen oxyanions participate in the reaction, although infrared spectra[12] indicate that such species are not present on the active catalyst. Single crystal data obtained under ultrahigh vacuum conditions provide valuable basic information. They show that NO dissociates completely on both smooth and stepped Cu surfaces[14−18] accompanied by facile desorption of N_2 and incipient oxidation of the metal. This suggests that at much higher reactant pressures it is unlikely that Cu^0 metal sites survive in a net oxidizing environment. Key information regarding the oxidation state of alumina-supported Cu catalysts under reaction conditions at atmospheric pressure comes from an in situ X-ray absorption near-edge structure (XANES) study carried out by Fernandez-Garcia et al.[19] Their results indicate that both Cu^+ and Cu^{2+} sites participate in the overall process, with Cu^+ being involved in the rate-limiting step.

Here we report on the electrochemical promotion (EP) by Na of the CO + NO reaction over a copper film catalyst supported on Na β'' alumina solid electrolyte, which acts as the source of electropumped spillover Na. This is the first time that EP has been observed with a base metal catalyst. The results shed light on the chemical composition of the catalytically active surface and on the way in which this composition varies as the CO/NO ratio varies from net reducing to net oxidizing conditions. In addition, we address certain aspects of the reaction mechanism and identify the chemical state of the Na promoter. In agreement with London and Bell[12] it is found that Cu nitrate is not present on the active surface. In agreement with Fernadez-Garcia et al.,[19] we show that the latter consists of Cu(I) and Cu(II) oxides, at least within the sampling depth of the X-ray photoelectron (XP) spectra (∼1 nm). Comparison with our earlier EP study of the Pt-catalyzed CO + NO reaction[20] is instructive and allows conclusions to be drawn about active sites and the mechanism of promotion in the Cu system.

Experimental Methods

The Cu catalyst (working electrode, W) consisted of a porous, continuous thin film deposited on one face of a 10 mm × 10 mm × 1.5 mm wafer of Na β'' alumina solid electrolyte. Au reference (R) and counter (C) electrodes were deposited on the other face, all three electrodes being deposited by Cu or Au sputtering in argon.[21] XPS analysis of the as-deposited Cu electrode showed a measurable C 1s signal (binding energy of 284 eV) corresponding to a submonolayer quantity of carbon. After exposure to reaction gas, the C 1s intensity was reduced

* To whom correspondence should be addressed.. Phone: 44 1223 336467. Fax: 44 1223 336362. E-mail: RML1@cam.ac.uk.

10.1021/jp992270d CCC: $18.00
Published on Web 10/26/1999

to an undetectable level. The surface area of the Cu catalyst working electrode (W) was estimated by measuring galvanostatic transients in a He atmosphere, as described in detail elsewhere.[21] The sample was suspended in a quartz, atmospheric pressure well-mixed reactor (50 cm^3) with all electrodes exposed to the reactant gas mixture. The system behaved as a single pellet, continuous stirred tank reactor (CSTR) as described and discussed elsewhere.[22]

Inlet and exit gas analysis was carried out by a combination of on-line gas chromatography (Shimadzu-14B; molecular sieve 5A and Porapak-N columns) and on-line mass spectrometry (Balzers QMG 064). N_2, N_2O, CO, and CO_2 were measured by gas chromatography, and NO was monitored continuously by mass spectrometry after performing the required calibrations. Reactants were pure NO (Distillers MG) and CO (Distillers MG) diluted in ultrapure He (99.996%) and fed to the reactor by mass-flow controllers (Brooks 5850 TR). The total flow rate was kept constant in all experiments at 6.8×10^{-5} mol s^{-1} (100 cm^3 (STP)/min), with partial pressures P_{NO} and P_{CO} of 0.5−6 and 1.5−2.5 kPa, respectively, and P_{He} giving a total pressure of 1 atm in every case. Conversion of the reactants was restricted to <15% in order to avoid mass transfer limitations. Control experiments were carried out in which the total flow was varied by a factor of 2 in order to verify that the observed changes in activity were due to actual changes in surface reaction rates and not due to mass transfer limitations. Nitrogen and carbon mass balances always closed to within 2%.

A galvanostat−potentiostat (Ionic Systems) was used to maintain a potential difference between the working and reference electrodes (potentiostatic mode). All experiments were carried out in potentiostatic mode by following the effect of catalyst potential (V_{WR}, measured with respect to the reference electrode) on the reaction rates.

Postreaction XPS measurements were carried out in a VG ADES 400 ultrahigh vacuum spectrometer system equipped with a reaction cell. The EP sample was mounted on a manipulator that allowed translation between the reaction cell and the spectrometer chamber. The sample holder was made from a machinable ceramic containing embedded Nichrome filaments for resistive heating, and all electrical connections were made with gold wire. XP spectra were acquired with Mg Kα radiation, constant pass energy of 20 eV, and with the Cu working electrode held at ground potential. Quoted binding energies are in reference to the Au $4f_{7/2}$ line at 83.8 eV, emitted by the Au wire used to make the electrical connection to the working electrode.

Results

Effect of Catalyst Potential (V_{WR}) on Reaction Rates. Figures 1−3 show steady-state (potentiostatic) rate data for CO_2, N_2, and N_2O production as a function of catalyst potential (V_{WR}) at 648 K for a range of reactant gas compositions determined by (fixed) inlet pressures (P^0_{NO}, P^0_{CO}) as follows: (Figure 1) $P^0_{CO} = 2.5$ kPa, $P^0_{NO} = 0.5$ kPa (CO/NO = 5:1); (Figure 2) $P^0_{CO} = 2$ kPa, $P^0_{NO} = 1$ kPa (CO/NO = 2:1); (Figure 3) $P^0_{CO} = 1.5$ kPa, $P^0_{NO} = 6$ kPa (CO/NO = 1:4). Turnover frequencies (TOF) are expressed as molecules of product per Cu surface atom per second. Also shown in Figures 1−3 is the dependence of N_2 selectivity on catalyst potential, where selectivity is defined as

$$S_{N_2} = \frac{r_{N_2}}{r_{N_2} + r_{N_2O}} \qquad \text{(I)}$$

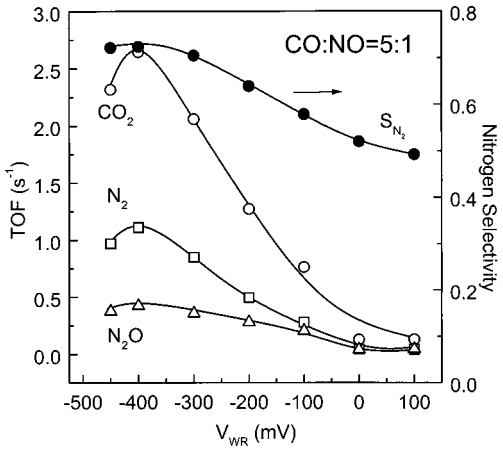

Figure 1. Effect of catalyst potential (V_{WR}) on the CO_2, N_2, N_2O formation rates and the selectivity of NO reduction to nitrogen. Conditions are $T = 648$ K, CO/NO = 5:1.

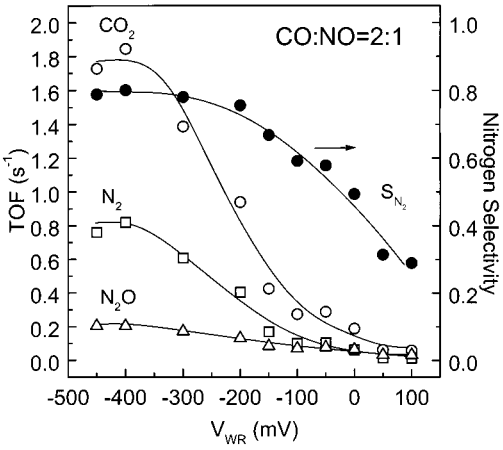

Figure 2. Effect of catalyst potential (V_{WR}) on the CO_2, N_2, N_2O formation rates and the selectivity of NO reduction to nitrogen. Conditions are $T = 648$ K, CO/NO = 2:1.

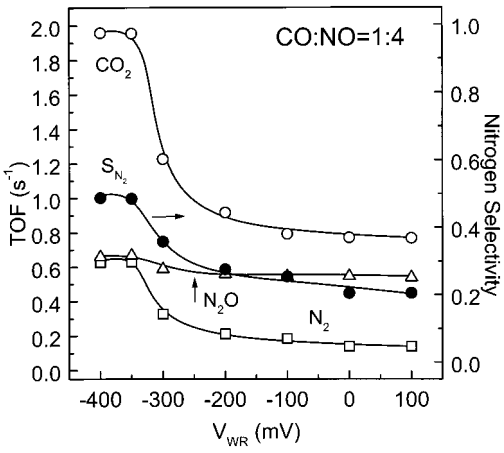

Figure 3. Effect of catalyst potential (V_{WR}) on the CO_2, N_2, N_2O formation rates and the selectivity of NO reduction to nitrogen. Conditions are T = 648 K, CO/NO = 1:4.

These data show that all rates (CO_2, N_2, and N_2O) increase with decreasing V_{WR}, which corresponds to progressively increasing the sodium loading of the Cu catalyst surface. Two features are evident: (i) for values of V_{WR} between 100 and −100 mV the reaction rates are almost constant (unpromoted regime) and (ii) there is a sharp increase in activity as V_{WR} is reduced below −100 mV (promoted regime). This behavior was reproducible and fully reversible. The rate enhancement ratios (ρ) defined

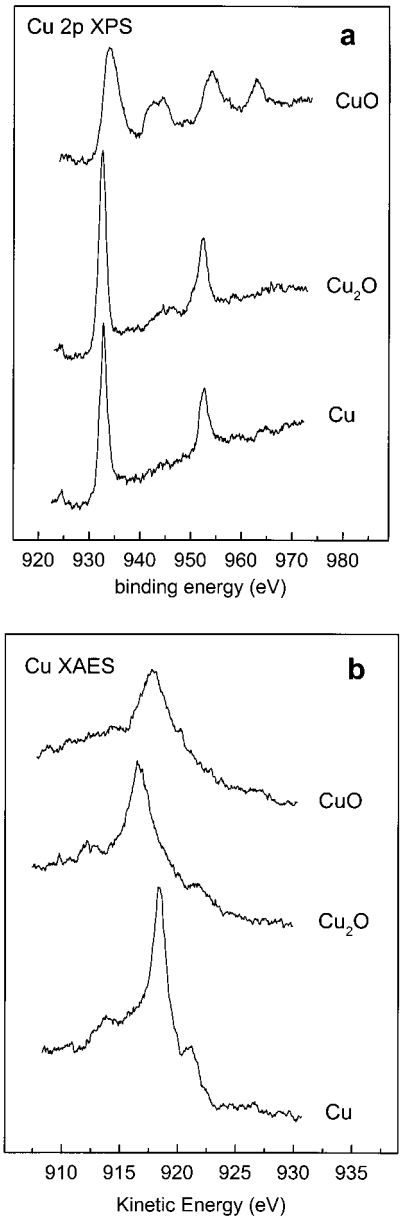

Figure 4. (a) Cu 2p XPS and (b) Cu LMM XAES for metallic Cu, Cu_2O, and CuO.

as the ratio of the maximum promoted rates r to the unpromoted rates r_0 are as follows for the three cases shown: (1) $\rho(CO_2) = 20$, $\rho(N_2) = 26$, $\rho(N_2O) = 11$, (2) $\rho(CO_2) = 26.4$, $\rho(N_2) = 66$, $\rho(N_2O) = 8.8$, and (3) $\rho(CO_2) = 2.5$, $\rho(N_2) = 4.4$, $\rho(N_2O) = 1.2$. It is apparent that decreasing V_{WR} not only caused substantial increases in all reaction rates but also caused appreciable enhancement of the nitrogen selectivity in every case: (a) from 50% to 75%, (b) from 29% to 80%, and (c) from 20% to 50%. (Note that the behavior observed at the stoichiometric composition CO/NO = 1:1 was very similar to that found for CO/NO = 2:1, namely, $\rho(CO_2) = 16$, $\rho(N_2) = 34$, $\rho(N_2O) = 3.2$; $S(N_2)$ increased from 25% to 75%.)

Postreaction XPS Studies of the EP Catalyst. XPS and Auger spectra were acquired after sample transfer to the electron spectrometer chamber following exposure to appropriate reaction gas environments in the reactor cell. For comparison purposes, we acquired reference Cu 2p XP and Cu LMM Auger electron (AE) reference spectra for Cu, Cu_2O, and CuO using the procedure described by Poulston et al.[23] These are illustrated in Figure 4. Postreaction XP/AE spectra were obtained after exposing the catalyst film to the same conditions of temperature and reactant partial pressures as those used in the CST reactor. During exposure of the catalyst to the reaction mixture, the V_{WR} conditions were such that the Cu film was either (i) unpromoted or (ii) Na-promoted. The spectra were acquired by the following procedure. (i) After exposure to reaction gas at the appropriate temperature, the sample was cooled to 330 K in reaction gas. (ii) Open-circuit conditions were imposed when the sample temperature was below 350 K, i.e., when Na mobility was low. The object of this procedure was to "freeze out" the surface conditions pertaining to the catalytically active surface.

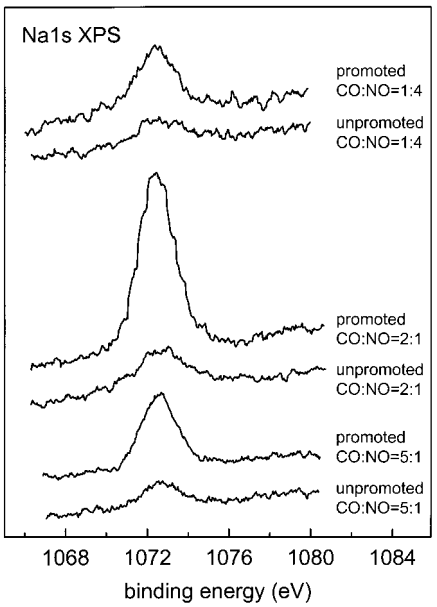

Figure 5. Na 1s XP spectra of the catalyst film after exposure to different reaction mixtures. The results refer to unpromoted and promoted conditions for different CO/NO ratios: (i) CO/NO = 5:1, (ii) CO/NO = 2:1, and (iii) CO/NO = 1:4.

These postreaction XP/AE experiments were performed in order to shed light on several important issues. (i) What evidence is there for the reversible transport of Na between electrolyte and catalyst under reaction conditions? (ii) What differences in catalyst surface composition are there between the unpromoted and promoted regimes? (iii) What surface species are formed by Na pumping to the Cu catalyst at reaction temperature in the presence of the reactant gases? (iv) What is the oxidation state of the Cu catalyst? We therefore exposed the sample to the same conditions as those used in the reactor, all at 648 K, 1 bar total pressure, as follows: (i) CO/NO = 5:1, (ii) CO/NO = 2:1, and (iii) CO/NO = 1:4 under unpromoted (V_{WR} = +100mV) and promoted (V_{WR} = −400mV) conditions. After these gas exposures the sample was transferred to the spectrometer chamber, as described above, and the XP spectra recorded.

A combination of Cu XP and X-ray excited Auger electron (XAE) spectra is required in order to distinguish between Cu metal, Cu_2O, and CuO.[11,23] Thus, CuO is characterized by high-intensity shake-up satellites at ~9 eV higher binding energy than the main $2p_{3/2}$ and $2p_{1/2}$ peaks. Additionally, the CuO main lines are shifted 1.2 eV toward higher binding energy and broadened compared to Cu_2O and Cu metal.[24] Cu metal and Cu_2O are best distinguished by their X-ray excited Cu LMM Auger spectra, since their Cu 2p transitions differ by only ~0.2 eV. We therefore recorded appropriate reference spectra, and these data are shown in Figure 4.

Figure 5 shows Na 1s XP spectra of the catalyst film taken after exposure to three different reaction mixtures under both

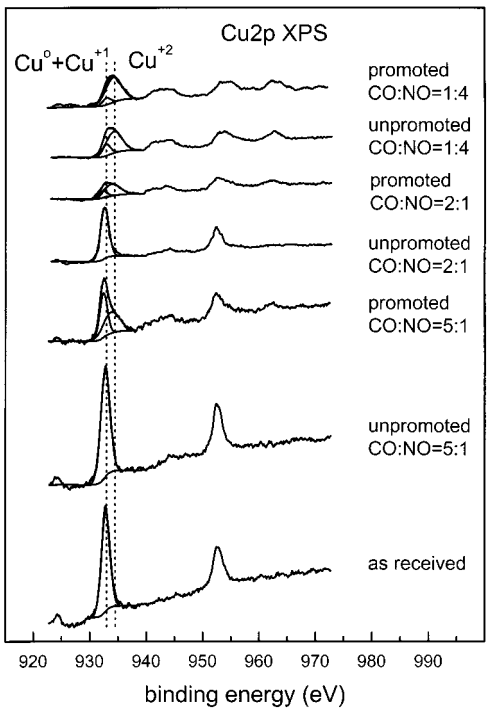

Figure 6. Cu 2p postreaction XP spectra of the catalyst film after exposure to the following CO/NO ratios: (i) CO/NO = 5:1, (ii) CO/NO = 2:1, and (iii) CO/NO = 1:4 for unpromoted and promoted conditions.

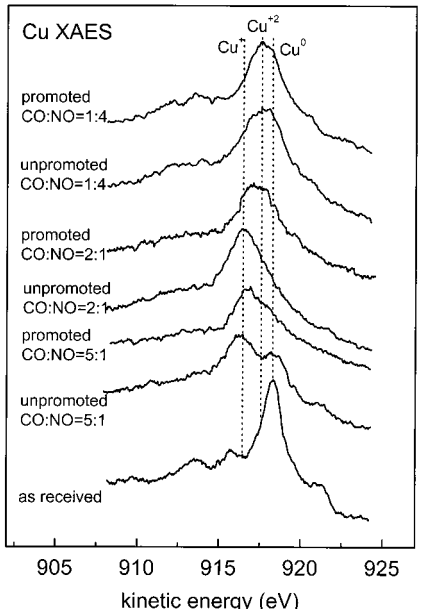

Figure 7. Cu LMM postreaction XAE spectra of the catalyst film after exposure to the following CO/NO ratios: (i) CO/NO = 5:1, (ii) CO/NO = 2:1, and (iii) CO/NO = 1:4 for unpromoted and promoted conditions.

unpromoted and promoted conditions. These results clearly demonstrate that the value of V_{WR} is directly correlated with the loading of Na on the catalyst surface under reaction conditions: decreasing the catalyst potential ($V_{WR} = -400$mV) causes an increase in the amount of Na. It is important to note that these spectral changes were fully reversible as a function of catalyst potential.

Analogous Cu 2p XPS and Cu LMM Auger spectra are shown in Figures 6 and 7, respectively. Several features are apparent from Figures 6 and 7 and may be summarized as follows: (1) initially, before use, the surface of the catalyst film consists of metallic Cu alone; (2) for a given catalyst potential, as the CO/NO ratio decreases (i.e., as the gaseous environment becomes more oxidizing), the oxidation state of the copper increases; (3) for a given CO/NO ratio, as the sodium coverage increases, the oxidation state of the copper is increased. Thus, the bottom spectra of Figures 6 and 7 show the Cu 2p and Cu LMM XAES spectra of the catalyst "as received". The sharp peak present at ~918.5 eV kinetic energy in the Cu LMM spectra and the shape and binding energy positions of the Cu $2p_{3/2}$ and Cu $2p_{1/2}$ demonstrate that the initial oxidation state of the Cu in the catalyst is zero, as comparison with the reference spectra in Figure 4 confirms. Exposing this "as-received" film to the same conditions of pressure and temperature as those used in the CST reactor with CO/NO = 5:1 *under unpromoted conditions* causes an increase in oxidation state of the Cu catalyst. The catalyst consists of Cu metal and Cu_2O as determined from the relevant Cu 2p XP and Cu LMM XAES spectra. Exposing the Cu film under the same initial conditions as before to the same gas environment and temperature but under *promoted* conditions causes a further increase in the oxidation state of the Cu film. In this case, the catalyst surface consists of Cu_2O and CuO. The same general trends were observed when the procedure was repeated with gas composition CO/NO = 2:1. In this case, the unpromoted catalyst consists of Cu_2O, whereas under promoted conditions the catalyst surface consists of Cu_2O and CuO, *no Cu^0 being detectable*. With CO/NO = 1:4 the unpromoted surface consists of CuO and a small amount of Cu_2O; the promoted surface consists almost entirely of CuO. These findings are summarized in Table 1. Quantification was achieved by estimating the integrated intensity of the Cu^0, Cu^+, and Cu^{2+} components and by assuming that (i) the photoionization cross section of Cu 2p is independent of oxidation state and (ii) the sampled volume is unaffected by the state of oxidation of the Cu film. Although these are not gross approximations, the estimated compositions should be regarded as no more than indicative.

TABLE 1: Determination of Surface Oxidation State Using Cu 2p XP and Cu LMM XAE Spectra[a]

	unpromoted (+100 mV)	promoted (−400 mV)
CO/NO = 5:1	$Cu^0 + Cu_2O$ (48% + 52%)	$Cu_2O + CuO$ (67% +33%)
CO/NO = 2:1	Cu_2O (100%)	$Cu_2O + CuO$ (28% + 72%)
CO/NO = 1:4	$Cu_2O + CuO$ (19% + 81%)	$Cu_2O + CuO$ (13% + 87%)

[a] Spectra acquired after exposure of the catalyst to the stated CO/NO ratios for values of V_{WR} corresponding to the promoted and unpromoted catalyst.

Figures 8 and 9 show the O 1s XP spectra and N 1s XP spectra, respectively, taken after exposing the film to exactly the same range of conditions as those pertaining to Figures 6 and 7. It is evident that (i) in all the unpromoted cases the O 1s signal exhibits only one feature at 530 eV binding energy and (ii) when sodium is present on the surface, a second feature appears at 532.5 eV binding energy. The 530 eV may be attributed with confidence to the oxides of copper[25] present on the surface under both unpromoted and promoted conditions. No carbonate species were present as judged by the complete absence of C 1s emission. Since the O 1s peak at 532.5 eV appeared only when sodium was present on the surface, we assign it to a sodium compound. We now show that this compound is $NaNO_3$.

Figure 9 shows relevant N 1s XP spectra; this signal was detectable at all CO/NO ratios but only after the catalyst had

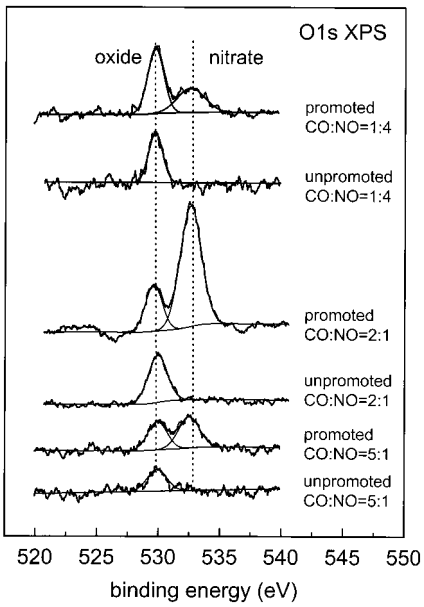

Figure 8. O 1s postreaction XP spectra of the catalyst film after exposure to the following CO/NO ratios at reaction temperature for unpromoted and promoted conditions: (i) CO/NO = 5:1, (ii) CO/NO = 2:1, and (iii) CO/NO = 1:4.

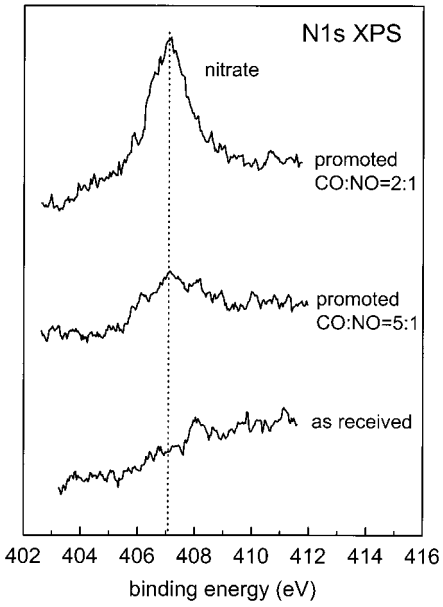

Figure 9. N 1s postreaction XP spectra of the catalyst film after exposure to the following CO/NO ratios at reaction temperature for unpromoted and promoted conditions: (i) CO/NO = 5:1, (ii) CO/NO = 2:1, and (iii) CO/NO = 1:4.

been run under promoted conditions. The binding energy (407 eV) corresponds to sodium nitrate.[26] Moreover, in any given case, the ratio of the intensity of the O 1s higher binding energy component to that of the corresponding N 1s emission was 2.86 (after normalization to account for photoionization cross section[27]). This provides strong quantitative support for the view that under promoted conditions sodium is present on the surface as $NaNO_3$. The binding energies observed in the Cu 2p spectra rule out the presence of copper nitrate[28] under all conditions. Heating the promoted catalyst in vacuum to 483 K causes the disappearance of both the higher binding energy O 1s signal and the N 1s peak, commensurate with the thermal stability of sodium nitrate.

Discussion

Given the lack of sensitivity of the CO + NO reaction toward the details of surface structure,[14−18] it is reasonable to take the view that our data and those obtained with conventional dispersed catalysts should be interpretable on the same general basis.

It is useful to summarize the overall pattern of behavior illustrated in Figures 1−3. First, regardless of reaction gas composition and Na loading, sodium promotion always leads to enhancement of both activity and N_2 selectivity. Second, the Na-induced enhancement in activity is very large under reducing conditions ($\rho \approx 20$ for CO/NO = 5:1 and 2:1) and an order of magnitude smaller under oxidizing conditions ($\rho = 2.5$, CO/NO = 1:4). Third, on the clean surface ($V_{WR} = +100$ mV) the nitrogen selectivity decreases with decreasing CO/NO ratio. Fourth, under the most reducing conditions, there is some retardation of all rates at the most negative potential (highest Na loading) for CO/NO = 5:1 but none when the reaction gas is more NO-rich.

Origin of Na Promotion and Nature of the Active Sites. The spectroscopic data show clearly that promotion is associated with the pumping of Na to the catalysts surface (Figure 5). They also establish that under reaction conditions (i) this sodium is present as the nitrate (Figures 8 and 9), (ii) no alkali carbonate is formed, (iii) no copper nitrate is present, and (iv) the promoted catalyst surface consists of Cu oxides. In view of (iii) we rule out participation of Cu nitrate in the overall catalytic process, in agreement with London and Bell[12] and at variance with Dekker et al.[13]

In our earlier work on NO reduction by CO[20] or propene[29] over platinum, we proposed that EP results from acceleration of the key reaction-initiating step: dissociation of adsorbed NO. In the case of a pure metal surface, we argued as follows. As the catalyst potential is decreased (pumping Na to the surface), the electronic effect of the sodium promoter on adsorbed NO strengthens the metal−N bond (increasing NO coverage) and weakens the N−O bond (facilitating NO dissociation). These effects are well understood and have been discussed in detail by Lang et al.[30] They are caused by the electric field of the alkali cation, which lowers the energy of the π^* orbital in the adjacent diatomic molecule. Increased electron density in the π^* orbital (i) strengthens the metal−N bond, thus increasing NO coverage, and (ii) facilitates dissociation of the N−O bond. These effects operate together to produce large increases in both activity and selectivity as a result of accelerating reaction 1 and inhibiting reaction 4:

$$NO_a \rightarrow N_a + O_a \qquad \text{promoted by Na} \tag{1}$$

$$N_a + N_a \rightarrow N_2 \tag{2}$$

$$CO_a + O_a \rightarrow CO_2 \tag{3}$$

$$NO_a + N_a \rightarrow N_2O \qquad \text{inhibited by Na} \tag{4}$$

It is worth noting that guided by these earlier EP results,[20,29] we synthesized conventional dispersed Pt/alumina catalysts that, when optimally promoted by Na, exhibited very large enhancements of both activity and selectivity for NO reduction by propene[31] and under simulated exhaust gas conditions.[32]

What happens in our case, which is complicated by the effects of Cu metal oxidation? There is little agreement in the literature regarding the question of which types of Cu sites are involved in catalytic turnover and which types of site adsorb NO, CO, or other possible adsorbates under reaction conditions. For

example, on the basis of their transient isotope reactor measurements, Dekker et al.[13] concluded that strongly bound NO is associated with Cu^+ sites. This is at variance with the proposal by Fu et al.,[33] based on low-temperature IR data, that CO and NO adsorb on both Cu^+ and Cu^{2+}, with NO adsorbed somewhat more strongly on Cu^{2+} and CO adsorbed somewhat more strongly on Cu^+. London and Bell[12] invoke Cu^0, Cu^+, and Cu^{2+} in the process of catalytic turnover; most other authors consider that only Cu^+ and Cu^{2+} sites are involved. Our results cannot resolve all these issues, but they do provide answers to some of them. As argued below, they demonstrate that Na promotion of NO dissociation is pivotal and accounts for the observed effects of EP on activity and selectivity in a natural way. In addition, they clearly demonstrate that the chemical composition of the active surface is strongly dependent on the composition of the reaction gas mixture, an issue that previously has not been investigated systematically. We therefore suggest that in the present case the reaction mechanism and mode of promotion are analogous to those proposed to explain the behavior of Pt catalysts undergoing EP of NO reduction.[20,29]

The postreaction XP and Auger spectra (Figures 6 and 7) indicate that the promoted surface does not contain detectable Cu^0. It consists of a mixture of Cu^{2+} and Cu^+ sites; the number density of the latter is relatively small under strongly oxidizing conditions, being detectable only in the Auger spectra. This is in line with the observations of Fu et al.[33] whose IR/XPS data obtained with CuO/alumina catalysts indicated the simultaneous presence of Cu^{2+} and Cu^+ at the surface. We therefore propose that the reaction is triggered by the Na-induced dissociation of NO adsorbed on Cu^+. Cu^+ rather than Cu^{2+} is suggested as the principal site for NO activation on the grounds of its finite 3d electron density. This d electron density should favor NO dissociation on Cu^+ (relative to Cu^{2+}) and thus should enhance the effect of Na promotion. This view is supported by the observation that the effects of Na promotion on both selectivity and activity are most pronounced *when the Cu^+ content of the clean (unpromoted) surface are highest* (Figures 1−3, 6, 7 and Table 1). It is also in accord with the findings of Fernandez-Garcia et al.,[19] whose XANES data led them to conclude that NO adsorption and dissociation at Cu^+ sites is the rate-limiting step for the unpromoted reaction. Formally, we may write

$$Cu^+{-}NO + Cu^+ \rightarrow Cu^+{-}N + Cu^{2+} + O^-$$

or

$$Cu^+{-}NO + 2Cu^+ \rightarrow Cu^+{-}N + 2Cu^{2+} + O^{2-}$$

The postreaction O 1s XP spectra favor the second possibility in that they show the presence of only O^{2-}. However, given the limitations of the method, O^- cannot be entirely ruled out.

The identity of the NO activating site(s) deserves further comment. Shelef and Gandhi have shown[34] that NO adsorbs faster at Cu^{2+} sites than it does at Cu^+ sites and that the adsorption enthalpy in the former case is a strongly decreasing function of coverage. Preferential adsorption of NO at Cu^{2+} sites may be rationalized in terms of the unpaired spins on adsorbate and adsorbent.[34] Our suggestion is based on adsorbed NO acting as a σ donor and π acceptor. Recent calculations[35,36] show that NO does indeed bond to Cu^+ by a σ/π mechanism and that the strength of the bond (~200 kJ) is not greatly different from that of the $Cu^{2+}{-}NO$ adsorption bond (~260 kJ).[37] With respect to mechanism, a key issue is the activation enery to dissociation of NO on the two types of Cu site. The weight of theoretical[30] and experimental evidence[33,38] suggests that this quantity should be lowest on Cu^+, consistent with our model. Thus, the observation[38] of a substantially lower N−O stretching frequency (1765 cm^{-1}) for $Cu^+{-}NO$ than for $Cu^{2+}{-}NO$ (1880 cm^{-1}) points to a reduced activation energy for NO dissociation in the former case. However, we cannot lose sight of the fact that the measured[34] and calculated[35,37] adsorption energies of NO on Cu^{2+} differ by a factor of 4. Clearly, further experimental and theoretical work is necessary in order to reconcile this apparent divergence.

Note that our results do not permit any conclusions to be drawn about the adsorption sites for CO. In passing, we note that an additional role of Na is that it catalyzes the oxidation of Cu by NO, thus accelerating formation of the active oxidized surface. Therefore, on balance, we agree with Fernandez-Garcia et al.[19] that the process of catalytic turnover may be written as follows:

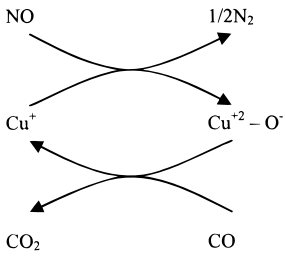

Figures 1−3 show that the nitrogen selectivity of the unpromoted (V_{WR} = +100 mV) catalyst decreases while decreasing the CO/NO ratio. This may be rationalized as follows. The mode of NO chemisorption on Cu^0, Cu^+, and Cu^{2+} is linear bonding through the nitrogen atom. The conventional view of this process is the donation/back model involving the π^* level of NO and d orbitals of the metal. Net electron transfer may thus vary from $NO^{\delta+}{-}M^{\delta-}$ to $NO^{\delta-}{-}M^{\delta+}$. On this basis, and in agreement with observation,[14−17] one expects the efficacy of Cu species for NO dissociation to lie in the order $Cu^0 > Cu^+ > Cu^{2+}$. The spectroscopic data show that decreasing the CO/NO ratio causes an increase in overall oxidation state of the copper. This in turn should result in a decrease in NO dissociation and hence a decrease in nitrogen selectivity.

Why Is There No Strong Poisoning at Negative V_{WR}? The behavior observed here bears interesting similarities to and differences from that observed for Pt[20] and Rh[39] surfaces undergoing EP by Na. In all three cases, there are large increments in both activity and selectivity under the influence of electropumped Na. Also, in all three cases, there is no tendency toward strong poisoning at the most negative values of catalyst potential that could be achieved. In this latter respect, the CO + NO reaction differs markedly from the propene + NO reaction on Pt[29] and Rh[40] and from propene combustion on Pt[41] under EP by Na. In these three cases, a region of strong promotion is followed by a regime of strong poisoning as the catalyst potential is decreased; small amounts of Na cause promotion and sufficiently large amounts of Na result in poisoning. Our XP spectra for CO + NO/Cu provide a basis for understanding this previously unexplained difference in behavior. The strongly poisoned systems result from overloading the catalyst with Na while propene is undergoing oxidation either by NO or by O_2. XP and XANES data show very clearly that, under such conditions, oxidation of this carbon-rich molecule leads to formation of thick films of Na carbonate that cover the surface and are stable at reaction temperature. This is consistent with the thermal properties of Na carbonate (melting point 1124 K). On the other hand, the present results clearly show that when

CO is oxidized by NO (a more facile reaction than propene oxidation), there is no formation of Na carbonate. Instead, the promoter phase consists exclusively of $NaNO_3$. Thick films of $NaNO_3$ (i.e., possessing the thermal properties of bulk sodium nitrate) would become volatile at ~580 K, decomposing altogether at ~650 K, which is the reaction temperature used in the present work. Submonolayer films of $NaNO_3$, however, would be expected to be more stable than the bulk material because of their strong interaction with the metal's surface. The very strong stabilization of two-dimensional films of ionic compounds adsorbed on metal surfaces relative to their three-dimensional analogues has been demonstrated[42] by experiment. Thus, in the present case, submonolayer quantities of $NaNO_3$ survive at reaction temperature, promoting the system. Thick films cannot be built up because of their volatility. As a result, strong poisoning does not occur. Note that there is some retardation (~10%) of the reaction rate at the highest Na loadings in CO-rich gas (CO/NO = 5:1). This may reflect onset of the formation of a more stable surface compound under these conditions. A possible cause for this retardation could be formation of a stable alkali−CO surface complex of the type detected on a number of different surfaces.[43]

Conclusions

(1) In the catalytic reduction of NO by CO, the reactive behavior, surface composition, and response to electrochemical promotion of Cu film catalysts are a strong function of the composition of the reactant gas, consistent with a redox mechanism.

(2) Under reducing or fairly oxidizing conditions the Cu-catalyzed CO + NO reaction exhibits strong electrochemical promotion of both activity and selectivity. Under strongly oxidizing conditions, promotion is still observed, but the effects are much less pronounced.

(3) The spectroscopic data indicate that these effects are due to pumping of Na to the catalyst where, under reaction conditions, it is present as $NaNO_3$ on an oxidized Cu surface. Na_2CO_3 and Cu nitrate are not detectable.

(4) The spectroscopic and reactor data indicate that Cu^0 sites are not of catalytic significance. In this regard, the weight of evidence suggests that Cu^+ is the principal site for NO adsorption and dissociation. EP is due to Na-induced enhancement of the adsorption and dissociation of NO at these sites.

Acknowledgment. F.J.W. acknowledges the award of a scholarship by Fundación YPF. Financial support from the U.K. Engineering and Physical Sciences Research Council and from the European Union is gratefully acknowledged under Grants GR/M76706 and BRPR-CT97-0460, respectively.

References and Notes

(1) Taylor, K. *Catal. Rev. Sci. Eng.* **1993,** *35*, 457.
(2) Shelef, M.; Otto, K. *J. Catal.* **1968**, *10*, 408.
(3) Shelef, M.; Otto, K.; Gandhi, H. *J. Catal.* **1968**, *12*, 361.
(4) Shelef, M. *Catal. Rev. Sci. Eng.* **1975**, *11*, 1.
(5) Parvulescu, V. I.; Grange P.; Delmon, B. *Catal. Today* **1998**, *46*, 233.
(6) Hildebrand, H. H.; Lintz, H.-G. *Appl. Catal.* **1990**, *65*, 241.
(7) Hildebrand, H. H.; Lintz, H.-G. *Catal. Today* **1991**, *9*, 153.
(8) Hildebrand, H. H.; Lintz, H.-G. *Ber. Bunsen-Ges. Phys. Chem.* **1991**, *95*, 1191.
(9) Bruck, J.; Brust, M.; Lintz, H.-G. *Ber. Bunsen-Ges. Phys. Chem.* **1995**, *99*, 1509.
(10) Estenfelder, M.; Lintz, H.-G. *Stud. Surf. Sci. Catal.* **1997**, *110*, 981.
(11) Jernigan, G. G.; Somorjai, G. A. *J. Catal.* **1994**, *147*, 567.
(12) London, J. W.; Bell, A. T. *J. Catal.* **1973**, *31***,** 96.
(13) Dekker, F. H. M.; Kraneveld, S.; Bliek, A.; Kapteijn, F.; Molelijn, J. A. *J. Catal.* **1997**, *170*, 168.
(14) Balkenende, A. R.; Gijzeman, O. L. J.; Geus, J. W. *Appl. Surf. Sci.* **1989**, *37*, 189.
(15) Balkenende, A. R.; den Daas, H.; Huisman, M.; Gijzeman, O. L. J.; Geus, J. W. *Appl. Surf. Sci.* **1991**, *47*, 341.
(16) Balkenende, A. R.; Hoogendam, R.; de Beer, T.; Gijzeman, O. L. J.; Geus, J. W. *Appl. Surf. Sci.* **1992**, *55*, 1.
(17) Balkenende, A. R.; van der Gift, C. J. G.; Meulenkamp, E. A.; Geus J. W. *Appl. Surf. Sci.* **1993**, *68*, 161.
(18) Wee, A. T. S.; Lin, J.; Huan, A. C. H.; Loh, F. C.; Tan, K. L. *Surf. Sci.* **1994**, *304*, 145.
(19) Fernandez-Garcia, M.; Marquez Alvarez, C.; Rodriguez-Ramos, I.; Guerrero-Ruiz, A.; Haller, G. L. *J. Phys. Chem.* **1995**, *99*, 16380.
(20) Palermo, A.; Lambert, R. M.; Harkness, I. R.; Yentekakis, I. V.; Marina, O.; Vayenas, C. G. *J. Catal.* **1996**, *161*, 471.
(21) Tracey, S.; Palermo, A.; Holgado Vazquez, J. P.; Lambert, R. M. *J. Catal.* **1998**, *179*, 231.
(22) Yentekakis, I. V.; Bebelis, S. *J. Catal.* **1992**, *137*, 278.
(23) Poulston, S.; Parlett, P. M.; Stone, P.; Bowker, M. *Surf. Interface Anal.* **1996**, *24*, 811.
(24) Leiro, J. A.; Heinonen, M. H.; Werfel, F.; Nordstrom, E. G.; Karlsson, K. H. *Philos. Mag. Lett.* **1993**, *68*, 153.
(25) Parmigiani, F.; Pachioni, G.; Illas, F.; Bagus, P. S. *J. Electron Spectrosc. Relat. Phenom.* **1992**, *59*, 255.
(26) Allen, H. C.; Laux, J. M.; Vogt, R.; Finlayson-Pitts, B. J.; Hemminger, J. C. *J. Phys. Chem.* **1996**, *100*, 6371.
(27) Yeh, J. J.; Lindau, I. *At. Data Nucl. Data Tables* **1985**, *32*, 1.
(28) Wagner, C. D. In *Practical Surface Analysis by Auger and X-ray Photoelectron Spectroscopy*; Briggs, D., Seah, M. P., Eds.; J.Wiley and Sons: New York, 1983.
(29) Yentekakis, I. V.; Palermo, A.; Filkin, N. C.; Tikhov, M. S.; Lambert, R. M. *J. Phys. Chem B* **1997**, *101*, 3759.
(30) Lang, N. D.; Holloway, S.; Norskov, J. K. *Surf. Sci.* **1985**, *150*, 24.
(31) Konsolakis, M.; Nalbantian, L.; McLeod, N.; Yentekakis, I. V.; Lambert, R. M. *Appl. Catal.* B, in press.
(32) Macleod, N.; Isaac, J.; Konsolakis, M.; Yentekakis, I. V.; Lambert, R. M. Manuscript in preparation.
(33) Fu, Y.; Tian, Y.; Lin, P. *J. Catal.* **1991**, *132*, 85.
(34) Gandhi, H. S.; Shelef, M. *J. Catal.* **1973**, *28*, 1.
(35) Casarin, M.; Maccato, C.; Vittadini, A. *Chem. Phys. Lett.* **1997**, *280*, 53.
(36) Casarin, M.; Vittadini, A. *Surf. Sci.* **1997**, *387*, L1079.
(37) Duan, Y. H.; Zhang, K. M.; Xie, X. D. *Surf. Sci.* **1994**, *321*, L249.
(38) Sepúlveda, A.; Márquez, C.; Rodriguez-Ramos, I.; Guerrero-Ruiz, A.; Fierro, J. L. *Surf. Interface Anal.* **1993**, *20*, 1067.
(39) Williams, F. J.; Palermo, A.; Tikhov, M. S.; Lambert R. M. Manuscript in preparation.
(40) Williams, F. J.; Palermo, A.; Tikhov, M. S.; Lambert, R. M. Manuscript in preparation.
(41) Filkin, N. C.; Tikhov, M. S.; Palermo, A.; Lambert, R. M. *J. Phys. Chem. A* **1999**, *103*, 2680.
(42) Lambert, R. M.; Kitson, M. *Surf. Sci.* **1981**, *110*, 205.
(43) Bertolini, J. C.; Delichere, P.; Massardier, J. *Surf. Sci.* **1985**, *160*, 331.